Design and testing of multi-PMTs and Regression Studies for New Generation Water Cherenkov Detectors

Brenda E. Medina[1,a], Elías A. Avendaño[1,b], Rajesh R. Biswal[1,c], Karen S. Caballero-Mora[3,d], Edgar Chucuan[1,e], Eduardo De la Fuente[2,f], Giannina Dalle Mese[4,g], Luis E. Falcón-Morales[1,h], Christoper E. Falcón Anaya[1,i], Rodrigo Gamboa-Goni[1,j], Elrick E. Haces Gil[1,k], Rodrigo Medina[1,l], Felipe Orozco-Luna[2,m], Gilberto Rodriguez[1,n], Lázaro M. Salas-Valtierra[2,o], Rodrigo Salmón-Folgueras[1,p], Alejandro K. Tomatani-Sánchez[1,q] and Saul Cuen-Rochin[1,r]

1 Tecnologico de Monterrey, Escuela de Ingenieria y Ciencias.
2 Departamento y Licenciatura de Fisica, CUCEI, Universidad de Guadalajara.
3 Facultad de Ciencias en Física y Matemáticas, Universidad Autónoma de Chiapas.
4 Facultad de Ciencias de la Tierra y el Espacio, Universidad Autónoma de Sinaloa.

a elisa_medina@exatec.tec.mx b a00833869@tec.mx c rroshanb@tec.mx
d karen.mora@unach.mx e edgar.chucuan@tec.mx f eduardo.delafuente@academicos.udg.mx
g giannina@uas.edu.mx h luis.eduardo.falcon@tec.mx i christopher.falcon@tec.mx
j r.gamboa@tec.mx k a00833699@tec.mx l roymedina@exatec.tec.mx m felipe.orozco@udg.mx
n a01635693@tec.mx o lazaro.salas0881@alumnos.udg.mx p jrsalmon@tec.mx
q katsumi@tec.mx r saulcuen@tec.mx

ISVHECRI 2024 Puerto Vallarta, México 8 -12 July

22nd International Symposium on Very High Energy Cosmic Ray Interactions (ISVHECRI 2024) Puerto Vallarta, Mexico, 8-12 July 2024
doi:10.21468/SciPostPhysProc.?

Abstract

This paper presents contributions to the mechanical-electronic design and testing of a multi-PMT (mPMT) vessel for the Hyper-Kamiokande (HK) experiment. Results of the computational and physical tests are satisfactory, pointing to potential areas for improvement. A regression study for reconstructing neutrino kinematic variables for the Intermediate Water Cherenkov Detector (IWCD) is also presented, using a ResNet-50 architecture; these findings help to improve neutrino precision detection methodologies.

Received Date
Accepted Date
Published Date

1 Introduction

Hyper-Kamiokande (HK) [1] is a state of the art international particle physics project focusing on neutrino detection and the study of fundamental particle interactions[1]. The development and testing of mPMTs [2] for HK is crucial to ensuring their proper functioning under ultra-pure water and high pressure conditions, and to detecting neutrino interactions through the

[1]To know more refer to the proceedings *Hyper-Kamiokande* by S. Cuen-Rochin.

emission of Cherenkov light radiation. This proceeding focuses on the improvement of the structural design, testing, and fabrication of a mPMT, together with a regression analysis to reconstructing kinematical variables using the Intermediate Water Cherenkov Detector (IWCD), a sub-detector from the HK observatory complex that, as well as the far detector (FD), will have its internal walls populated with strings of arrays of mPMTs.

2 IWCD Regression Studies

Systematic uncertainty reduction in HK demands old and new detectors to be repurposed and constructed, respectively [3] [4]. IWCD is a novel cylindrical water tank detector (8 m in length and 7 m in width), capable of vertically moving through a pit to measure neutrino fluxes at different off-axis angles. The mPMT populated detector, can contain muons with up to 1 GeV/c, providing a comprehensive measurement capability [5]. This study uses Particle Gun (PG) data and a Neutrino Beam Sample (NBS) dataset. PG data is generated using WCSim[2], simulating simple interactions where some of the associated kinematic variables are uniformly distributed. In contrast, NBS data shows complex distributions, better reflecting real-world conditions. ResNet (Residual Neural Network) is a convolutional architecture that uses skip connections to facilitate the training of deep networks and mitigate the vanishing gradient problem [6]. Multiple ResNet-50 models were trained on PG data for electron and muon events, with separate models for each kinematic variable; position, direction and energy, and particle type μ and e^-. The performance of these models was then evaluated using the NBS dataset. Events were selected to evaluate model performance where the energy is less than 1 GeV above the Cherenkov threshold, a minimum of 25 hits, and a minimum distance of 50 cm between the vertex position and the detector wall. A fiTQun[3] flag was also applied to indicate whether the particles were fully contained in the detector. The range in kinematic variables covered by this event selection matches well the PG dataset used during the training stage. Additionally, the model's performance was evaluated across various charged-current interaction channels: Charged-Current Quasi-Elastic (CCQE) - the purely quasielastic interaction (1p1h), two-particle two-hole (2p2h) emission channel, and finally the Single Pion Production (SPP, CC1π).

After evaluating the model, a performance comparison is obtained based on residual histograms (figure 1). The model consistently achieves better reconstruction performance for the PG data set as compared to the NBS data. Among the different CC-interaction channels, the model performs best for the golden channel category (1p1h); predictions for the 2p2h category are reasonably accurate, while CC1π events are consistently predicted poorly across all variables. A plausible explanation for this behavior is that CCQE events are simpler, involving fewer particles, whereas CC1π events typically produce multiple rings[4], increasing the complexity of the event, making accurate reconstruction more difficult for the model.

3 Mechanical Design, Simulation and Testing of the mPMT module

A stress analysis (buckling and deformation simulations) was performed in SolidWorks using a mPMT 3D model (figure 2-a) to evaluate the effects of different materials and stress types over the vessel components (figure 2-b), and identify potential mechanical design improvements. A key simulation, the stress test, revealed areas where the device experiences high stress due

[2] https://github.com/WCSim/WCSim

[3] Legacy software used in Super-Kamiokande

[4] Signal events appear as ring-like structures visible within the internal walls of the IWCD.

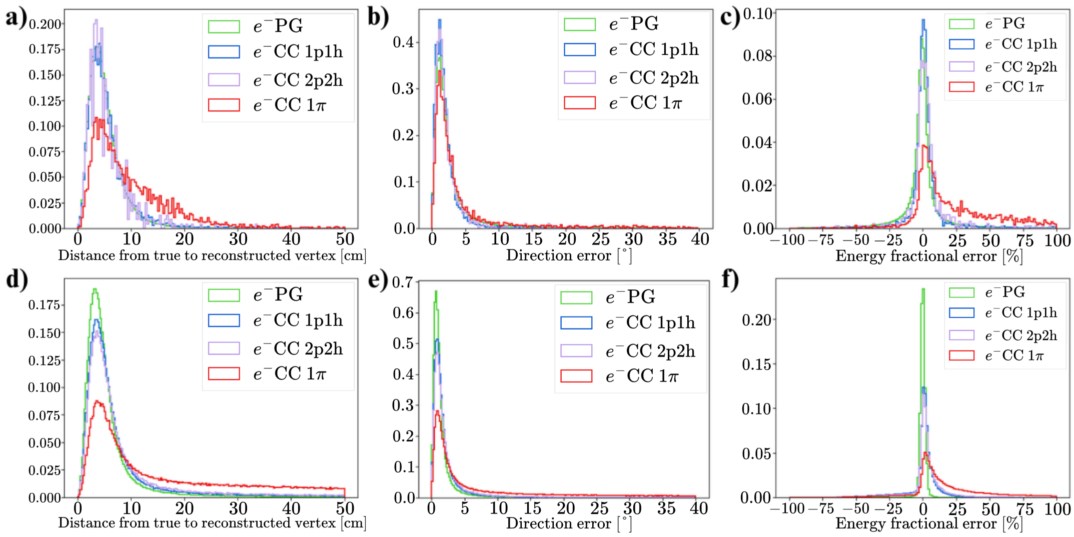

Figure 1: Reconstruction error residuals for e^- (top row), and μ (bottom row) events using PG and NBS, for distance (left), direction (center) and energy (right).

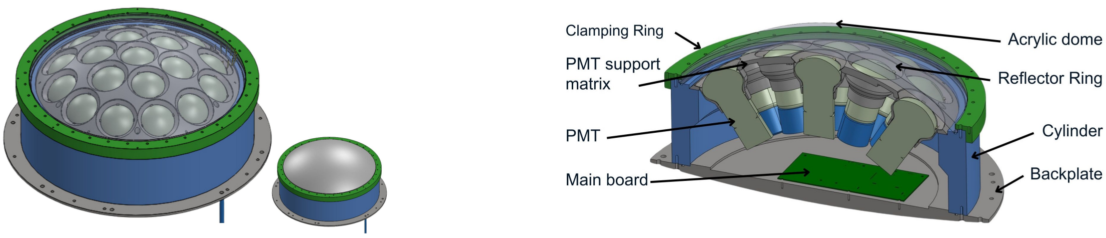

(a) (b)

Figure 2: (a) mPMT SolidWorks 3D model. (b) Schematic of the mPMT.

47 to hydrostatic pressure (70 m of water column), as indicated by the color scale in figure 3.

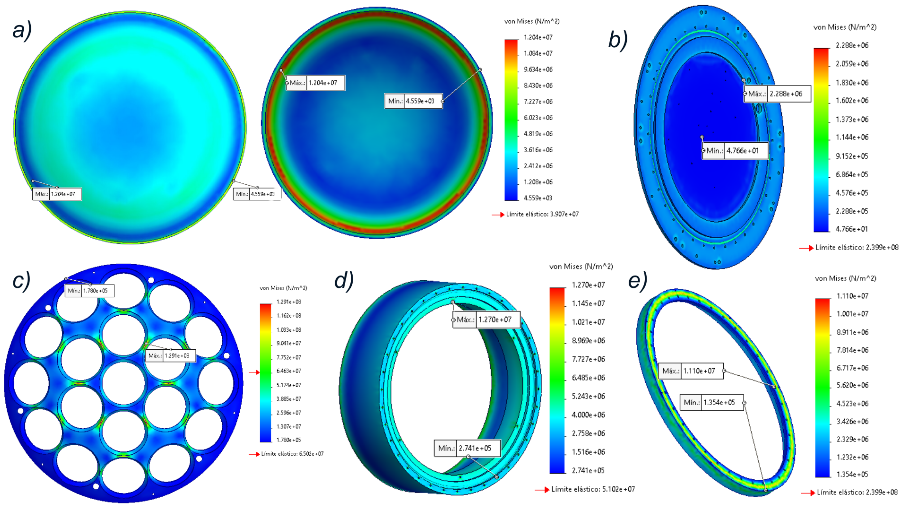

Figure 3: Von Mises stress results for the different objects, for a simulated water depth of 70 m. a) Top and bottom of Plaskolite General Purpose Acrylic Resin Dome. b) Backplate of AISI-316 material. c) PMT vessel of ABS material. d) Cylinder of POM-C material. e) Clamping Ring of AISI-316 material.

The most affected components were the Acrylic Dome and the mPMT vessel. The bottom edge of the Acrylic Dome, which has an elastic limit of $3.907 \times 10^7\ N/m^2$, experienced a maximum stress of $1.204 \times 10^7\ N/m^2$. This value, while significant, remains below the elastic limit of the material. In contrast, the mPMT vessel experienced a maximum stress of $1.291 \times 10^8\ N/m^2$ at the joints, exceeding the ABS material's elastic limit of $6.502 \times 10^7\ N/m^2$. Although the mPMT vessel is not directly exposed to hydrostatic pressure, the joints are vulnerable and may require reinforcement to prevent structural failure. To address these issues, additional computational simulations were conducted for each component using nine alternative materials, to identify more resistant options. Table 1 summarizes the materials that best withstand hydrostatic pressure based on the aforementioned simulations.

Component	**Original material**	**Best material**		
		Buckling test	**Stress test**	**Deformation test**
Dome	Plexiglas GS-UVT	General Purpose Acrylic Resin	Röhm ACRYLITE	Both
PMT vessel	ABS, PET-G and resins	ABS (ABS834G40L)	PET-G	
Cylinder	POM-C	Stainless steel AISI-304		
Backplate	AISI-304	Stainless steel AISI-316		
Clamping Ring				

Table 1: Results of best materials for each component.

3.1 Metrology and testing of the mPMT base design

A metrology study of the mPMT´s vessel components was carried out to verify the dimensional accuracy for the 3D printing of the vessel's PMT support matrix. Physical measurements of the prototype were compared to the SolidWorks model, with a margin of error below 1% [7]. Of the 416 collected measurements, most absolute errors between the measured and reference dimensions, fell within the specified tolerance, confirming the validity of the 3D printing PMT support matrix. Furthermore, the Mexican collaboration designed and constructed mPMT support structure prototypes for the barrel, top, and bottom configurations of Hyper-K's main tank Inner Detector (ID). Such structures were put to the test via simulating earthquake frequencies, demonstrating the mechanical stability of the mPMT vessel in all configurations (top, bottom, and barrel) within the water tank, figure 4. In addition, packaging, transportation, and installation tests were performed to evaluate the durability of the associated designs under various conditions. Finally, vibration, compression, and humidity tests confirmed the prototype's packaging resistance to transportation stresses, including handling frequencies, stowage loads, and environmental humidity.

Figure 4: mPMT and support structures vibration test for the top, bottom and barrel positions.

3.2 Reflector ring results

An aluminum reflector ring prototype was designed and fabricated at Tecnológico de Monterrey, to evaluate an alternative manufacturing method. These rings are designed to increase the photosensitive area around the PMTs, improving their focused acceptance and providing additional directional information. Six two-dimensional prototypes of reflector rings were cut from a 25-gauge (0.46 *mm* thick) aluminum sheet using a plasma cutter. The resulting dimensions and angles were close to the design specifications; however, defects were found on the edges of the rings. This is likely attributed to factors associated with the cutting process[5].

4 Photonic Characterization of Aluminum Rings and PMTs

Within the HK project, characterization of the PMTs and their reflector rings is essential. This process requires the tuning of two systems: the electrical - for the PMT operation, and the optical - to control the emission of individual photons. The objective is quantifying the efficiency gains (if any), associated with the inclusion of the reflector rings.

Figure 5: Experimental setup: Black Box for Single Photon Emission with Weak Coherent Source and PMT (left). Electrical Pin-Outs (right).

The aluminum rings have shown to increase the PMT efficiency by 20%. COMSOL raytracing simulations yielded an efficiency increase of 15.8% for a single PMT, and 18.6% for the whole mPMT assembly. Using the experimental setup shown in Fig. 5, described in detail in the next section, we aimed at confirming the 15.8% increase in efficiency mentioned above, by experimentally counting the number of detected photons.

4.1 Electrical PMT Readout

A photomultiplier is connected to a Voltage Divider, distributing the voltage from a common HV supply to the individual dynodes [6] of the device. Each incident photon is converted into a photoelectron, amplified by the PMT gain, producing a charge pulse in the output. The number of detected photons can therefore be determined by counting the output pulses via an oscilloscope. Two types of voltage dividers were used: one specified by Hamamatsu for usage with PMTs R14374 and R14689, and a second one specified by the HK collaboration.

4.2 Single Photon Emission Optical Setup

A 402 nm laser, simulating Cherenkov emission, is attenuated to the single-photon regime using stacked neutral-density filters, targeting an overall optical density of ∼15 (from 1 mW to $\sim 5\times10^{-19}$ W, i.e., ∼1 photon/s at 402 nm). PMTs (e.g., Hamamatsu R14374/R14689) are read out on a digital oscilloscope using both the vendor and HK-specified dividers.

[5]Such as the parameters and maintenance condition of the plasma cutter.

[6]A specialized electrode found in vacuum tubes, that acts as an electron multiplier by emitting secondary electrons when struck by incident electrons.

4.3 Proposed Experimental Setup

To experimentally determine the efficiency gain from the aluminum reflector ring, we will measure photon counts with and without the ring in place. Using the single-photon emission setup from the last section, with the addition of a microscope objective lens, the 402 *nm* laser beam will be uniformly spread to illuminate the PMT photocathode. Finally, by comparing the integrated photon counts under these two conditions, we can quantify the efficiency enhancement. This measurement will allow us to verify the 20% gain reported in Hyper-K technical documents and corroborate the 15.8% increase predicted by COMSOL simulations.

5 Conclusion

Preliminary results for the mPMT vessel and support structures were satisfactory, establishing a solid foundation for future studies, and ensuring their structural resistance to working conditions under high hydrostatic pressure. Regarding the IWCD regression studies, results demonstrates the viability of employing deep learning models, particularly ResNet-50, to reconstruct muon and electron events for the IWCD. While ResNet-50 models show promise, particularly in analyzing distinct interaction types, future work should aim at improving performance for events with higher energy. Characterization-wise, the next steps will include single photon detection with Hamamatsu's R14374 PMT, and its associated mPMT array.

Acknowledgements

The authors would like to thank CONAHCyT projects CF-2023-G-643 and CBF2023-2024-427, for supporting this work.

References

[1] Hyper-Kamiokande Proto-Collaboration: K. Abe et al, *Hyper-kamiokande design report*, https://arxiv.org/abs/1805.04163 (2018).

[2] G. De Rosa, *A multi-pmt photodetector system for the hyper-kamiokande experiment*, Nuclear Instruments and Methods in Physics Research Section A: Accelerators, Spectrometers, Detectors and Associated Equipment **958**, 163033 (2020), doi:10.1016/j.nima.2019.163033, Proceedings of the Vienna Conference on Instrumentation 2019.

[3] N. W. Prouse, *The Intermediate Detector and Neutrino Phenomenology of the Hyper-Kamiokande Experiment*, Ph.D. thesis, Queen Mary, U. of London, http://qmro.qmul.ac.uk/xmlui/handle/123456789/46804 (2018).

[4] S. Cuen-Rochin, E. de la Fuente, L. Falcon-Morales, R. Gamboa Goni, A. K. Tomatani-Sanchez, F. Orozco-Luna, H. Torres, J. Lozoya, J. A. Baeza, J. L. Flores, B. Navarro-Garcia, B. Veliz *et al.*, *Machine Learning Application for Particle Physics: Mexico's Involvement in the Hyper-Kamiokande Observatory*, pp. 583–608, Springer International Publishing, Cham, ISBN 978-3-030-70542-8, doi:10.1007/978-3-030-70542-8_23 (2021).

[5] T. Zhu, *Long-baseline neutrino oscillation sensitivities with Hyper-Kamiokande and impact of Intermediate Water Cherenkov Detector*, In *Proceedings of Neutrino Oscillation Workshop — PoS(NOW2022)*, vol. 421, p. 028, doi:10.22323/1.421.0028 (2023).

[6] K. He, X. Zhang, S. Ren and J. Sun, *Deep residual learning for image recognition*, CoRR **abs/1512.03385** (2015), 1512.03385.

[7] S. Cuen-Rochin, *Multi-photomultiplier tube module development for the next generation hyper-kamiokande neutrino experiment*, In *International Workshop on Next generation Nucleon Decay and Neutrino Detectors*, https://indi.to/TjjMH (2019).